Heterogeneous & Homogeneous & Bio- & Nano-

CHEMCATCHEM

CATALYSIS

Accepted Article

Title: Multilayered Two-Dimensional V2CTx MXene for Methane Dehydroaromatization

Authors: Raj Thakur, Megan Hoffman, Armin VahidMohammadi, Justin Smith, Mingyang Chi, Bruce Tatarchuk, Majid Beidaghi, and Carlos Carrero

To be cited as: *ChemCatChem* 10.1002/cctc.201902366

Link to VoR: http://dx.doi.org/10.1002/cctc.201902366

A Journal of ChemPubSoc Europe

WILEY-VCH

www.chemcatchem.org

10.1002/cctc.201902366

WILEY-VCH

COMMUNICATION

Multilayered Two-Dimensional V_2CT_x MXene for Methane Dehydroaromatization

Raj Thakur, [a] Megan Hoffman, [a] Armin VahidMohammadi, [b] Justin Smith, [a] Mingyang Chi, [a] Bruce Tatarchuk, [a] Majid Beidaghi, [b] and Carlos A. Carrero*[a]

[a] R. Thakur, M. Hoffman, J. Smith, M. Chi, Dr. B.Tatarchuk, Dr. C.A.Carrero*
Department of Chemical Engineering
Auburn University
212 Ross Hall
E-mail: cac0134@auburn.edu

[b] Dr. A. VahidMohammadi, Dr. M. Beidaghi
Department of Materials Engineering
Auburn University
279 Wilmore laboratories

Supporting information for this article is given via a link at the end of the document.

Abstract: We report a thermally stable multilayered two-dimensional vanadium carbide (V_2CT_x) MXenes catalyst for the direct conversion of methane (CH_4) into benzene (C_6H_6). The multilayered carbide structure shows state-of-the-art CH_4 conversion 11.8% with a C_6H_6 formation rate of 1.9 mmol $g_{cat}^{-1}h^{-1}$ (4.84% C_6H_6 yield) at 700 ^{0}C, which is comparable to the benchmark Mo/ZSM-5 catalyst. The structure-activity relationship was explored by numerous characterization techniques including *in-situ/operando* Raman-MS, *ex-situ* X-ray diffraction (XRD), scanning electron microscopy (SEM), X-ray photoelectron spectroscopy (XPS), and ammonia temperature programmed desorption (NH_3-TPD). This work provides a new platform to design and explore multilayered two-dimensional catalysts demonstrating confinement effect to convert CH_4 into $*C_2H_3$ intermediates which further oligomerizes inside multilayered structures producing C_6H_6 as a final product.

Multilayered MXenes are a relatively new family of two-dimensional (2D) metal carbides and nitrides.[1] They are named by their graphene-like morphology, in accordance with the general chemical formula $M_{n+1}X_nT_x$, where *n* can be 1,2 , or 3, *M* is an early transition metal, *X* is carbon and/or nitrogen, *T* indicates various surface terminations ($^-$OH, O^- and F^-), which depend on the preparation method, and *x* is the number of surface functional groups per unit formula (Scheme S1).[2] Already, about 20 different MXenes have been synthetized, while the properties of several have been theoretically predicted.[1a, 3] Their potential and attractiveness reside on both their unique electronic and mechanical properties, and the bonding between interlayers which exhibits a combination of ionic, metallic, and covalent character.[1a, 4]

Only few studies have been reported on the catalytic activity of MXenes at relatively high temperatures, such as the ammonia perchlorate decomposition,[1a, 5] water gas shift reaction,[6] ethyl benzene dehydrogenation,[7] and propane dehydrogenation.[8] Based on the good thermal and chemical stability of *m*-V_2CT_x, especially under inert and reducing atmospheres,[9] we decided to further explore the catalytic properties of this material for the production of liquid aromatics via methane dehydroaromatization (MDA). Recently, we reported *m*-V_2CT_x as an active, selective and coke-resistant catalyst for the dry reforming of methane at 800 ^{0}C.[10] We proposed an *in-situ redox* mechanism that demonstrates the catalytic attractiveness of MXenes for reactions where deactivation by carbon deposition is still a present issue. Taking advantage and simultaneously combining the *i)* structure of multilayered MXenes, that eventually provides the confinement effect that has been proposed as responsible to enhance the selectivity toward aromatics when using zeolites,[11] *ii)* the oxy-carbide species coexisting on the surface of MXenes,[12] and *iii)* the relatively good thermal and structural stability of *m*-V_2CT_x under various conditions,[9] paved the path to study the MDA reaction over this promising *m*-V_2CT_x MXenes catalyst (Reaction 1).

$$6CH_4 \rightleftarrows C_6H_6 + 9H_2 \qquad (1) \qquad \Delta H^0_{298K} = 434 \text{ kJ mol}^{-1}$$

The MDA reaction has gained interest essentially due to *i)* the ever-growing demand of aromatics, *ii)* the lack of on-purpose technologies for the production of aromatics, driven by the recent trends of using shale gas as feedstocks in cracker units,[11d, 13] and *iii)* the notable discrepancies in the literature regarding the nature of active site(s) and the possible reaction mechanism when using the benchmark Mo/ZSM-5 catalysts.[14] The MDA process is far from industrial implementation due to stability-related issues as a result of various reasons such as *i)* rapid catalyst deactivation caused by carbonaceous deposits obstructing the catalytically active sites,[15] *ii)* extraction of framework Al species above 700ºC,[11c, 13a] *iii)* migration of the active site (Mo species) from internal to external framework in zeolites,[13a] *iv)* rapid increase in graphitic-amorphous carbon over TOS demanding severe regeneration processes,[16] and *v)* the lack of consensus about the nature of active sites whether they are oxidic (MoO_x), carbidic (MoC_x) and/or oxy-carbidic (MoC_xO_y).[14]

Herein, we report the use of *m*-V_2CT_x MXene as an active, selective, and potentially regenerable catalyst for MDA. We synthesize *m*-V_2CT_x by selectively etching Al from the corresponding precursor, so-called MAX phase (V_2AlC), using hydrofluoric acid (Scheme 1).[9, 17]

10.1002/cctc.201902366

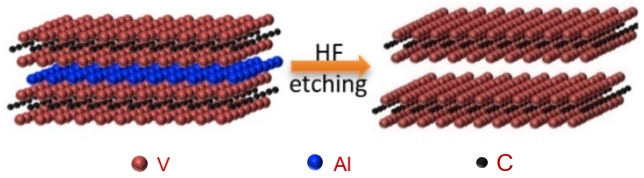

Scheme 1. Schematic representation of the V_2AlC MAX phase transformation into V_2CT_x MXene after HF treatment.

In line with the literature, we carried out the MDA reaction at 700ºC using 50 mol% of both methane (CH_4) and inert, primarily producing benzene and hydrogen.[18] As stated in various studies using the benchmarked Mo/ZSM-5 catalyst, the first step in MDA reaction involves the carburization of the catalyst,[11d, 19] wherein the molybdenum oxide, anchored in the internal framework of the zeolite, is converted to carbide/oxy-carbide, which then acts as the active site for converting methane.[11b, 11c, 13a, 14, 20]

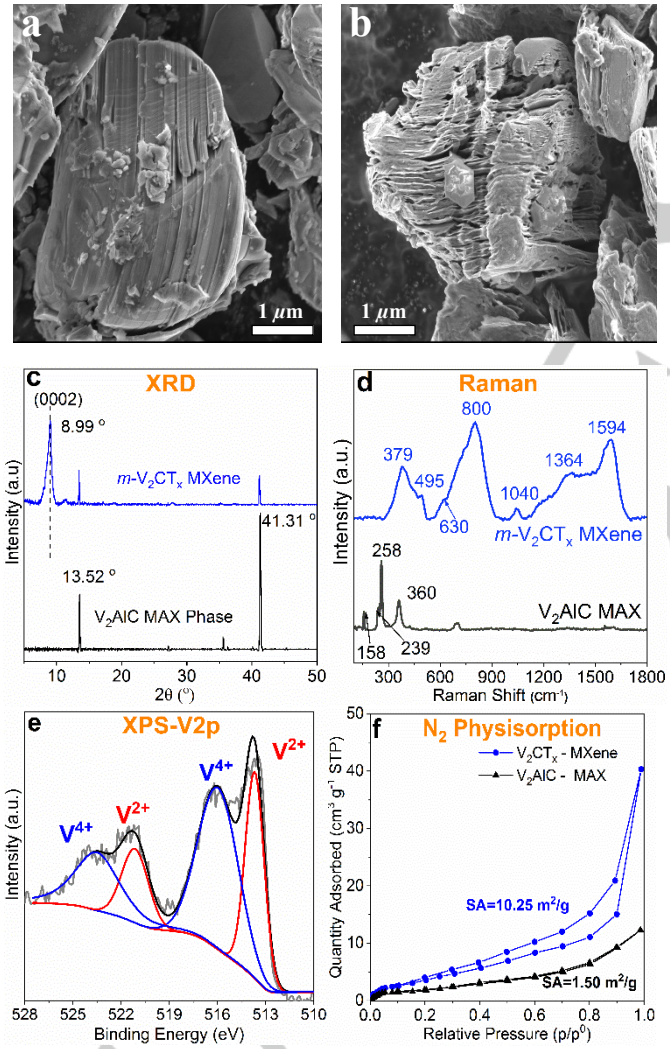

Figure 1. SEM micrograph of (a) V_2AlC MAX and (b) m-V_2CT_x MXene. (c-d) XRD diffractogram and Raman of V_2AlC MAX phase and the m-V_2CT_x MXenes. (JCPDS No. 29-0101). (e) XPS V2p spectra of as prepared m-V_2CT_x MXenes. (f) N_2 physisorption of V_2AlC MAX and m-V_2CT_x MXene. SA=Surface Area.

Initially, C-H bond activation occurs inside the channels of ZSM-5 forming methyl radicals, that subsequently dimerize forming C2 species and further undergoing oligomerization and cyclization over Bronsted acid sites to finally produce benzene (Scheme S2).[11a, 13a].

Scanning electron microscopy (SEM) confirms the formation of m-V_2CT_x MXene (Figure 1b) after HF-treatment of V_2AlC Max phase (Figure 1a). The precursor, V_2AlC, shows its typical morphology analogous to a tightly stacked un-exfoliated graphite as observed by scanning electron microscopy (SEM) (Figure 1a).[9, 17a] After the HF treatment, the tightly stacked layers transform to loosen accordion-like morphology with stacked layers well separated from each other due to the etching of Al atoms from MAX phase (Figure 1b).[9, 17a]

Interestingly, the well-defined layered structure provides an interlamellar space of ~ 7.0 Å,[9] which is slightly larger than the kinetic diameter of benzene (~ 6.0 Å).[11d, 18] These interlamellar spaces provide the confinement necessary for the oligomerization and cyclization of intermediates (C2 species) to then form benzene. X-ray diffraction (XRD) (Figure 1c) shows a characteristic peak at 2θ of 8.99° which corresponds to (0002) plane for m-V_2CT_x, along with traces of unreacted V_2AlC MAX phase (13.5° and 41.3°). The latter appears in almost all MXenes synthesized by HF etching, because more severe etching procedures lead to the extraction of V as well, resulting in forming carbide-derive-carbon (CDC) materials.[1a, 9] The Raman spectra (Figure 1d) for the V_2AlC MAX phase exhibits sharp peaks at 158 (E_{2g}), 239 (E_{2g}), 258 (E_{1g}), and 360 (A_{1g}) cm^{-1},[21] while for the m-V_2CT_x exhibits boarder peaks at 379, 495, 630, 800, 1040, 1364, and 1594 cm^{-1}. This broadening of peaks for m-V_2CT_x is attributed to the large interlayer spacing,[21c] and the assignment of all the Raman vibrations can be found elsewhere.[9] Amongst the various vibrations, the Raman peak at 800 cm^{-1} corresponds to two dimensional V_2CT_x MXene with terminal functional groups (F, OH),[21c] which typically appears around 750 cm^{-1} for bulk VC carbide.[21c] Also, we track the changes on the surface of m-V_2CT_x using X-ray photoelectron spectroscopy (XPS) (Figure 1e). The peak centered at ~513.3 eV (V^{2+}) evidences both the presence of unreacted V_2AlC MAX phase and the V-C phase from the V2p and C1s region, respectively. The peak centered at ~ 516.3 eV (V^{4+}) is attributed to the existence of a monolayer of vanadium oxide on the surface of vanadium carbide.[17a] Details of the deconvoluted XPS spectra in the C1s and O1s region be found in Figure S1. The N_2-physisorption study (Figure 1f) of m-V_2CT_x shows a surface area of 10.25 m^2/g and H3-type adsorption-desorption trajectory with a hysteresis loop (P/P_0 = 0.5-1.0) distinctive for macroporous and layered materials.[7] While the V_2AlC (MAX phase) has a surface area of 1.50 m^2/g and no porosity.

After confirming the formation of m-V_2CT_x, we explored its catalytic activity in MDA under industrially attractive conditions and specifically focused on benzene formation (Figure 2). As shown in Figure 2a, the rate of formation of C_6H_6 initially has a maximum formation rate of 1.9 mmol $C_6H_6/g_{cat}.h$ at 11.8 % CH_4 conversion, which decreases as a function of time up to 0.4 mmol $C_6H_6/g_{cat}.h$ in about ten hours. Similar deactivation trend is observed when using Mo/ZSM-5 catalyst (Figure S2), although with higher magnitude (2.3 to 1.1 mmol $C_6H_6/g_{cat}.h$ within seven hours). The C_6H_6 yield for both catalysts can be found in Figure S3.

10.1002/cctc.201902366

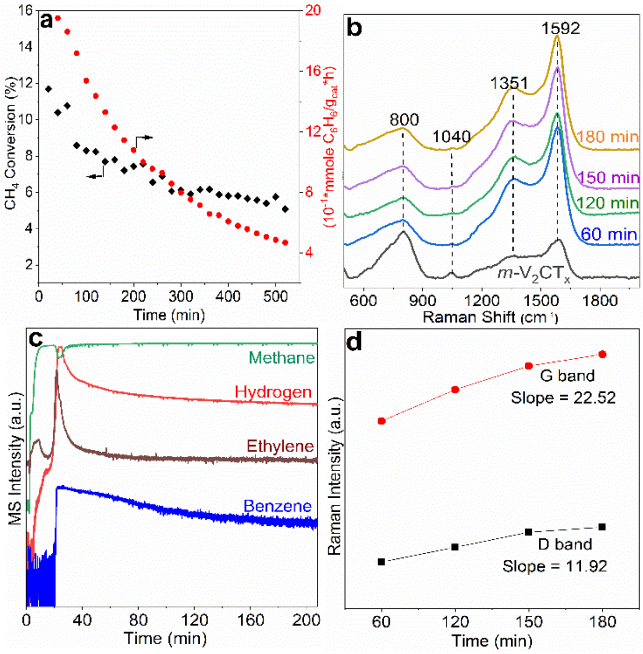

Figure 2. (a) CH_4 conversion and C_6H_6 formation rates over *m*-V_2CT_x MXene. (b-c) Operando Raman -MS plot (d) Relative rate of D (1351 cm^{-1}) and G (1592 cm^{-1}) carbon formation as a function of TOS at 700 ^{0}C.

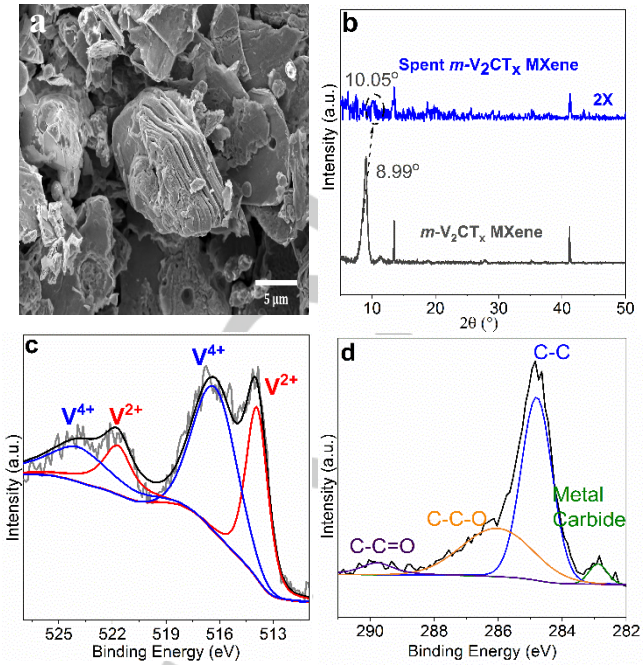

Figure 3. (a) SEM, (b) XRD, and XPS of spent *m*-V_2CT_x MXenes, evidencing the excellent structural and thermal stability.

On the other hand, the V_2AlC MAX phase exhibits no reactivity in MDA (Figure S4), thus proving the need of confinement to produce benzene.[11d]

Operand Raman spectroscopy, evidences *i)* the presence of the 2D structure of *m*-V_2CT_x (peaks at 800 cm^{-1} and 1040 cm^{-1} assigned to 2D-VC and 2D-V=O,[9] respectively) (Figure 2b), *ii)* the formation of C_2H_4 and H_2 as the initial products followed by the formation of C_6H_6 (Figure 2c), and *iii)* the development of solid amorphous and graphitic carbon on the surface (eventually in between the layers) of *m*-V_2CT_x (Figure 2b&d). Such carbonaceous species limit the accessibility of CH_4 inside the channels, explaining the deactivation. As the reaction proceeds, the amount of C_6H_6 starts to decrease (Figure 2a and c), which coincides with the rise of D/G carbon Raman peaks (Figure 2b). The D-carbon peak corresponds to the sp^3 amorphous carbon while the G-carbon peak is attributed to the sp^2 graphitic carbon.[9] The gradual drop in C_6H_6 can be attributed to precipitation of carbon (amorphous and graphitic) in between the layers, thereby blocking the active sites and ultimately reducing the activity of the catalyst. Figure 2c shows that the formation of coke starts right from the onset of MDA reaction as the C_6H_6 and H_2 signals starts to decre-ase.

We performed SEM, XRD, and XPS to the spent material to further explore the deactivation process. The SEM micrographs still shows up to certain extent the multilayered structure of the material (Figure 3a), while XRD reveals that the (0002) MXene peak remarkably decreases (noise level) and shift to a slightly higher angle (Figure 3b). The almost disappearance of this specific diffraction peak can be attributed to the deposition of carbon between the layers, while its shift is primarily due to a decrease in the lattice parameter because of dehydration.[9]

Finally, the V2p (Figure 3c) XPS spectra shows the presence of 516.3 eV (V^{4+}) and ~513.3 eV (V^{2+}) peaks, similarly to Figure 1e.

Additionally, the C1s spectra (Figure 3d) shows prominent C-C (~284.8 eV) along with V-C (~282.2 eV) peaks. The C-C (~284.8 eV) peak increases relative to V-C (~282.2 eV), confirming the deposition of carbon on the surface. The N_2 physisorption profile for the spent catalyst can be found in Figure S5, where the typical H3-type N_2 adsorption-desorption trajectory is observed.

As for Mo/ZSM-5 catalyst,[11, 13a, 14] we propose that first the CH_4 is activated over metal (V-C) sites of *m*-V_2CT_x MXene, thereby forming CH_x species, which further undergoes oligomerization and dimerization through a series of gas phase reactions in between the interlayers yielding C_6H_6, C_2H_4 and H_2. (Figure 4). Methyl and ethyl oligomerization primarily occurring in gas phase to yield benzene have already been reported when using Fe©SiO2 catalysts.[13b]

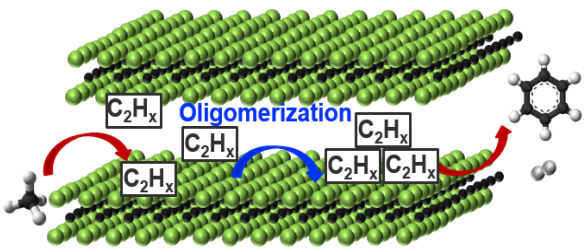

Figure 4. MDA reaction scheme over *m*-V_2CT_x MXene forming C_6H_6 and H_2 as the main reaction products.

However, the need of (weak) Lewis acid sites to catalyze the oligomerization of C2 species to form benzene has been also proposed.[22] *m*-V_2CT_x contains less, but still some, Lewis and Brönsted sites when comparing to Mo/ZSM-5 (Figure S6). Such acidity can be attributed to the presence of terminal functional groups (e.g. OH and O^-) and/or due to unreacted MAX Phase within the MXene. At this point, we cannot conclusively state that

solely the proposed gas-phase mechanism for MDA occurring in a confinement environment is taking place when using *m*-V_2CT_x, because it also contains acid sites, which might significantly contribute during the oligomerization of the ethyl radicals (*C_2H_3) to form benzene as proposed when using zeolite-based catalysts.[11a, 11d, 13a]

In summary, we have shown that *m*-V_2CT_x MXene catalyzes the formation of benzene via MDA at 700ºC with a maximum formation rate of 1.9 mmol C_6H_6/g_{cat}.h (4.84% C_6H_6 yield), which is comparable to state-of-the-art Mo/ZSM-5 catalysts (2.3 mmol C_6H_6/g_{cat}.h). We hope that this catalytic performance potentially encourages the heterogeneous catalysis community to explore the ever-growing family of MXenes in the upgrading of natural gas. The interesting properties observed by *in-situ/operando* Raman, *ex-situ* XRD, XPS and SEM for the pristine and spent *m*-V_2CT_x MXene, corroborate the remarkable and attractive stability of this material when comparing to metal-containing zeolite catalysts, which typically suffer from structural changes due to, for instance, the expulsion of aluminum ions from the zeolite lattice forming both octahedral non-framework aluminum ion and $Al_2(MoO4)_3$.[11d, 13a] However, *m*-V_2CT also deactivates due to the deposition of amorphous/graphitic carbon, which remains as one of the challenges for potential industrial application. The regeneration protocol required to remove carbon from spent catalysts, becomes an issue when using transition metal carbides materials because of their total-bulk oxidation.

Ongoing research in our group on the use of MXenes for catalytic applications at relatively high temperatures (>400 ^{0}C) has resulted in developing a protocol to remove carbonaceous species and avoiding total-bulk oxidation of the layered carbide phase.[10] Playing with various regeneration protocols, tuning the acidity of *m*-V_2CT_x, controlling the interlayer distance, and testing other MXenes phases (Scheme S1) are the follow-up strategies we are currently working on to gain new insights into the genesis of an alternative, suitable, and regenerable no-zeolite catalyst for MDA. Furthermore, since scaling-up the synthesis of MXenes is still an issue, primarily due to the high exothermicity of the process and the use of strong acids such as HF, we are currently applying a factorial experimental design to increase the production of multilayered MXenes per batch without altering the intrinsic material structure and properties.

There are over twenty different MXenes that have been synthetized so far, with different and tunable structures, properties, and surface terminations, which we envision are going to broaden the applicability of MXenes either as catalyst precursors, catalysts, or catalyst supports for suitable catalytic reactions.

Experimental Section

Synthesis of V_2AlC MAX phase

For the synthesis of V_2AlC, vanadium powder (99.5%, 325 mesh, Alfa Aesar), aluminum powder (99.5%, 325 mesh, Alfa Aesar), and graphite powder (99%, 325 mesh, Alfa Aesar) were mixed in a 2:1.3:1 ratio, which was the ball milled using zirconia balls for about 18 h. The mixture was then sintered at 1500 °C with a heating rate of 3 °C/min for 4 h under flowing inert argon atmosphere. The prepared MAX phases were further crushed, milled, and sieved through a 400 mesh to obtain powders with an average particle size of ~32 µm.

Synthesis of V_2CT_x MXene

To synthesize V_2CT_x MXene, V_2AlC MAX phase was treated with 48-50% concentrated hydrofluoric acid (ACS grade, BDH) in a ratio of 1g powder to 20 mL etchant and stirred with a Teflon-coated magnetic bar at 200 rpm for 92 h at room temperature. For more details, the detailed procedure can be found elsewhere.[4a, 17a, 23] Briefly, the etched powder was then washed several times using DI water and centrifuged at 3500 rpm for about 5 minutes until the pH of the supernatant was higher than four. The MXene powder was then filtered using a Celgard porous membrane, rinsed with DI water and absolute ethanol, collected, and dried under vacuum for 24h.

Acknowledgements

The authors acknowledge financial support from the Departments of Chemical and Materials Engineering at Auburn University. RT and A.V.M. acknowledge the support from Auburn CO_2 center and Alabama EPSCoR Graduate Research Scholar Program (GRSP Round 11 and 12) doctoral fellowships respectively. M.B. acknowledges the support from Auburn University's IGP program.

Conflict of interest

The authors declare no conflict of interest.

Keywords: heterogenous catalysis • carbides • kinetics • methane • 2D material • MXenes

[1] a) B. Anasori, M. R. Lukatskaya, Y. Gogotsi, *Nature Reviews Materials* **2017**, *2*, 16098; b) W. Choi, N. Choudhary, G. H. Han, J. Park, D. Akinwande, Y. H. Lee, *Materials Today* **2017**, *20*, 116-130.
[2] M. Naguib, M. Kurtoglu, V. Presser, J. Lu, J. Niu, M. Heon, L. Hultman, Y. Gogotsi, M. W. Barsoum, *Advanced Materials* **2011**, *23*, 4248-4253.
[3] J. Zhu, E. Ha, G. Zhao, Y. Zhou, D. Huang, G. Yue, L. Hu, N. Sun, Y. Wang, L. Y. S. Lee, C. Xu, K.-Y. Wong, D. Astruc, P. Zhao, *Coordination Chemistry Reviews* **2017**, *352*, 306-327.
[4] a) M. Naguib, J. Halim, J. Lu, K. M. Cook, L. Hultman, Y. Gogotsi, M. W. Barsoum, *Journal of the American Chemical Society* **2013**, *135*, 15966-15969; b) Z. Li, Y. Wu, *Small* **2019**, 1804736.
[5] Y. Gao, L. Wang, Z. Li, A. Zhou, Q. Hu, X. Cao, *Solid State Sciences* **2014**, *35*, 62-65.
[6] Z. Li, Y. Cui, Z. Wu, C. Milligan, L. Zhou, G. Mitchell, B. Xu, E. Shi, J. T. Miller, F. H. Ribeiro, *Nature Catalysis* **2018**, *1*, 349.
[7] J. Diao, M. Hu, Z. Lian, Z. Li, H. Zhang, F. Huang, B. Li, X. Wang, D. Su, H. Liu, *ACS Catalysis* **2018**, *8*, 10051-10057.
[8] Z. Li, L. Yu, C. Milligan, T. Ma, L. Zhou, Y. Cui, Z. Qi, N. Libretto, B. Xu, J. Luo, *Nature communications* **2018**, *9*, 5258.
[9] R. Thakur, A. VahidMohammadi, J. Moncada, W. R. Adams, M. Chi, B. Tatarchuk, M. Beidaghi, C. A. Carrero, *Nanoscale* **2019**, *11*, 10716-10726.
[10] R. Thakur, A. VahidMohammadi, J Smith, J. Moncada, M. Beidaghi, C. A. Carrero, 2019 (Submitted)
[11] a) A. Sridhar, M. Rahman, S. J. Khatib, *ChemCatChem* **2018**, *10*, 2571-2583; b) N. Kosinov, A. S. Wijpkema, E. Uslamin, R. Rohling, F. J. Coumans, B. Mezari, A. Parastaev, A. S. Poryvaev, M. V. Fedin, E. A. Pidko, *Angewandte Chemie International Edition* **2018**, *57*, 1016-1020; c) N. Kosinov, F. J.

Coumans, G. Li, E. Uslamin, B. Mezari, A. S. Wijpkema, E. A. Pidko, E. J. Hensen, *Journal of Catalysis* **2017**, *346*, 125-133; d) S. Ma, X. Guo, L. Zhao, S. Scott, X. Bao, *Journal of Energy Chemistry* **2013**, *22*, 1-20.
[12] B. Anasori, Y. Xie, M. Beidaghi, J. Lu, B. C. Hosler, L. Hultman, P. R. Kent, Y. Gogotsi, M. W. Barsoum, *ACS nano* **2015**, *9*, 9507-9516.
[13] a) J. Gao, Y. Zheng, J.-M. Jehng, Y. Tang, I. E. Wachs, S. G. Podkolzin, *Science* **2015**, *348*, 686-690; b) X. Guo, G. Fang, G. Li, H. Ma, H. Fan, L. Yu, C. Ma, X. Wu, D. Deng, M. Wei, D.Tan, R.Si, S.Zhang, J.Li, L.Sun, Z.Tang, X.pan, X.Bao, *Science* **2014**, *344*, 616-619; c) N. Kosinov, E. A. Uslamin, L. Meng, A. Parastaev, Y. Liu, E. J. Hensen, *Angewandte Chemie International Edition* **2019**, *58*, 7068-7072.
[14] I. Lezcano-González, R. Oord, M. Rovezzi, P. Glatzel, S. W. Botchway, B. M. Weckhuysen, A. M. Beale, *Angewandte Chemie International Edition* **2016**, *55*, 5215-5219.
[15] Y. Zhang, H. Jiang, *Chemical communications* **2018**, *54*, 10343-10346.
[16] Y. Song, Q. Zhang, Y. Xu, Y. Zhang, K. Matsuoka, Z.-G. Zhang, *Applied Catalysis A: General* **2017**, *530*, 12-20.
[17] a) A. VahidMohammadi, A. Hadjikhani, S. Shahbazmohamadi, M. Beidaghi, *ACS Nano* **2017**, *11*, 11135-11144; b) B. Anasori, Y. Gogotsi, in *2D Metal Carbides and Nitrides (MXenes)*, Springer, **2019**, pp. 3-12.
[18] I. Vollmer, I. Yarulina, F. Kapteijn, J. Gascon, *ChemCatChem* **2019**, *11*, 39-52.
[19] a) N. K. Razdan, A. Kumar, A. Bhan, *Journal of Catalysis* **2019**, *372*, 370-381; b) M. Rahman, A. Infantes-Molina, A. Boubnov, S. R. Bare, E. Stavitski, A. Sridhar, S. J. Khatib, *Journal of Catalysis* **2019**, *375*, 314-328.
[20] A. Sridhar, M. Rahman, A. Infantes-Molina, B. J. Wylie, C. G. Borcik, S. J. Khatib, *Applied Catalysis A: General* **2020**, *589*, 117247.
[21] a) V. Presser, M. Naguib, L. Chaput, A. Togo, G. Hug, M. W. Barsoum, *Journal of Raman Spectroscopy* **2012**, *43*, 168-172; b) J. E. Spanier, S. Gupta, M. Amer, M. W. Barsoum, *Physical Review B* **2005**, *71*, 012103; c) A. Champagne, L. Shi, T. Ouisse, B. Hackens, J.-C. Charlier, *Physical Review B* **2018**, *97*, 115439.
[22] M. F. Hsieh, Y. Zhou, H. Thirumalai, L. C. Grabow, J. D. Rimer, *ChemCatChem* **2017**, *9*, 1675-1682.
[23] A. VahidMohammadi, M. Mojtabavi, N. M. Caffrey, M. Wanunu, M. Beidaghi, *Advanced Materials* **2019**, *31*, 1806931.

10.1002/cctc.201902366

Entry for the Table of Contents

The transformation of CH_4 into C_6H_6 and H_2 over highly thermally stable multilayered two-dimensional structure, where the multilayer structure provides necessary confinement for the intermediate C2 radicals to produce C_6H_6.

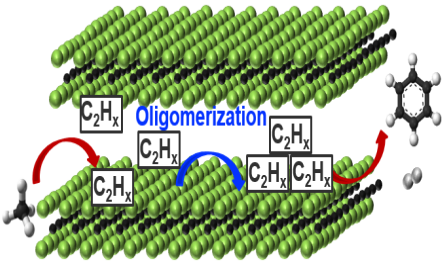

R. Thakur, M. Hoffman, A VahidMohammadi, J. Smith, M. Chi, B. Tatarchuk, M. Beidaghi, and C. A. Carrero*

Multilayered Two-Dimensional V_2CT_x MXenes for Methane Dehydroaromatization